TRAJECTORY TRACKING CONTROL OF MOBILE MANIPULATORS BASED ON KINEMATICS

Razvan Solea and Daniela Cernega
Departament of Automation and Electrical Engineering, "Dunarea de Jos" University of Galati
Domneasca Street, No.47, 800008 Galati, Romania

Keywords: Mobile manipulators, Nonlinear control, Kinematics.

Abstract: This paper focuses on the motion planning problem of mobile manipulator systems, i.e. manipulators attached on mobile platforms. The paper presents a methodology for generating trajectories for both the mobile platform and the manipulator that will take a system from an initial configuration to a pre-specified final one, without violating the nonholonomic constraint. The contributions of this paper come from the development and evaluation of sliding-mode control scheme for the composite wheeled robot that facilitate maintenance of all kinematic constraints within such systems. Given an arbitrary trajectory,the mobile-manipulator controller must generate a smooth desired trajectory for mobile platform.

1 INTRODUCTION

Mobile Manipulator systems are typically composed of a mobile base platform with one (or more) mounted manipulators. Taking advantage of the increased mobility and workspace provided by the mobile base, such systems have found applications in industry and in research principally due to their engineering simplicity (easy to build and to control than legged robots) and their low specific resistance (high energy efficiency). Moving mobile manipulators systems, present many unique problems that are due to the coupling of holonomic manipulators with nonholonomic bases.

Any system combining a wheeled mobile platform and one or several manipulators (classically arms) is named *wheeled mobile manipulators* (WMM) - like in Fig. 1. From the set of constraints and characteristics, different approaches have been developed to control WMM. A first class of approach is inherited from the control schemes that have been developed for manipulators. Those control schemes have been extended to WMM in order to account for their specificities. Among those approaches, the pioneering work of H. Seraji1 (Seraji, 1993) can be distinguished. He proposed an extension of kinematic based control laws to the case of a mobile manipulator equipped with a wheeled platform (unicycle) and a manipulator.

A variety of theoretical and applied control problems have been studied for various classes of nonholonomic control systems. Motion planning problems are concerned with obtaining open loop controls that steer the system from an initial state to a final state without violating the nonholonomic constraints.

Figure 1: Pioneer 3DX mobile robot with manipular.

The determination of the actuator rates for a given end effector motion of a redundant manipulator is typically an under-constrained problem. A number of schemes have been proposed in the literature for the resolution of the redundancy. The principal underlying theme is one of optimizing some measure of performance based on kinematics of the system and in some cases extended to include the dynamics. However, in this paper, we focus our attention purely on kinematic redundancy resolution schemes.

Solea R. and Cernega D..
TRAJECTORY TRACKING CONTROL OF MOBILE MANIPULATORS BASED ON KINEMATICS.
DOI: 10.5220/0003533200210027
In *Proceedings of the 8th International Conference on Informatics in Control, Automation and Robotics* (ICINCO-2011), pages 21-27
ISBN: 978-989-8425-75-1

The control algorithms and strategies have been categorized into three groups, namely continuous time-variant, discontinuous and hybrid control strategies (Kolmanovsky and McClamroch, 1995), (Tanner et al., 2003), (Sharma1 et al., 2010), (Murray, 2007), (Klancar et al., 2009), (Mazo et al., 2004), (Zavlanos and Pappas, 2008). Output tracking laws are easier to design and implement, and can be embedded in a sensorbased control architecture when the task is not fully known in advance. For this reason, with the exception of (Fruchard et al., 2005) that takes a somehow intermediate approach, most works on WMMs focus on kinematic control, e.g., (Bayle et al., 2002), (Luca et al., 2010), (Tang et al., 2008).

The rest of the paper is organized as follows: Section 2 develops the notation and the kinematic model for the WMM under consideration. Section 3 focuses on creation of a kinematic control law based on sliding-mode strategy. Section 4 presents simulation results to show the effectiveness of the trajectory-traking control scheme. Section 5 concludes the paper with a brief discussion and summarizes the avenues for future work.

2 KINEMATIC MODEL

In this section, we present the notation and the kinematic model of the system under consideration. Referring to Figure 2, the WMM under consideration consists of a differentially driven WMR base with a mounted planar two-link manipulator (is considered for simplity). The wheels are located at a distance of b from the center of the wheel axle. The wheel has a radius of r. The base of the manipulator is located at a distance of a D from the center of the wheel axle. The length of the first and second links are L_1 and L_2 respectively.

Motion planning has been treated mostly as a kinematic problem where the dynamics of the system have been generally neglected. However, with nonholonomic systems, ignoring the dynamics reduces the significance of the results to low speeds although it is well documented that avoidance of obstacles, parking maneuverability, and more motion control is feasible at higher speeds as well.

The configuration of a WMM can be completely described by the following generalized coordinates:

$$q^T = [x_R, y_R, \phi_R, \theta_1, \theta_2] \tag{1}$$

where $[x_R, y_R, \phi_R]$ describes the configuration of the WMR and $[\theta_1, \theta_2]$ describes the configuration of the planar manipulator. (x_R, y_R) is the Cartesian position of the center of the axle of the WMR, ϕ_R is

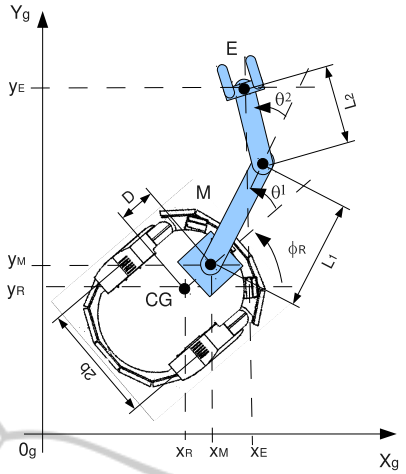

Figure 2: Schematic of the WMM.

the orientation of the WMR, and θ_2, θ_2 are the relative angles that parameterize the first and second link of the mounted manipulator. The kinematics of the differentially-driven WMR can be represented by its equivalent unicycle model, and described as:

$$\begin{aligned} \dot{x}_R &= v_R \cdot cos(\phi_R) \\ \dot{y}_R &= v_R \cdot sin(\phi_R) \\ \dot{\phi}_R &= \omega_R \end{aligned} \tag{2}$$

where v_R and ω_R are the forward and angular velocities inputs.

The position and orientation of the end-effector in the world frame can be derived from homogeneous transform according to the position and orientation of the mobile robot in the world frame, that of the end-effector in the manipulators base frame, and the transform between the mobile robot frame and the manipulators base frame. The kinematics of the mobile manipulator can be described like:

$$\begin{aligned} x_E &= x_M + L_1 \cdot cos(\phi_R + \theta_1) + L_2 \cdot cos(\phi_R + \theta_1 + \theta_2) \\ y_E &= y_M + L_1 \cdot sin(\phi_R + \theta_1) + L_2 \cdot sin(\phi_R + \theta_1 + \theta_2) \end{aligned} \tag{3}$$

where (x_M, y_M) is the position of mounting point M of the mobile platform and ϕ_R is the platform orientation. Eqs.3 show that the position of the end-effector E depends on the position and the orientation of the mobile platform. This illustrates the fact that mobile manipulators, in contrast to fixed ones, can have an infinite workspace.

$$\begin{aligned} x_M &= x_R + D \cdot cos(\phi_R) \\ y_M &= y_R + D \cdot sin(\phi_R) \end{aligned} \tag{4}$$

By differentiating eqs. (3) and (4) will get:

$$\begin{aligned}\dot{x}_E &= v_R \cdot cos(\phi_R) - D \cdot \omega_R \cdot sin(\phi_R) - \\ &- L_1 \cdot (\omega_R + \omega_1) \cdot sin(\phi_R + \theta_1) \\ &- L_2 \cdot (\omega_R + \omega_1 + \omega_2) \cdot sin(\phi_R + \theta_1 + \theta_2) \\ \dot{y}_E &= v_R \cdot sin(\phi_R) + D \cdot \omega_R \cdot cos(\phi_R) + \\ &+ L_1 \cdot (\omega_R + \omega_1) \cdot cos(\phi_R + \theta_1) \\ &- L_2 \cdot (\omega_R + \omega_1 + \omega_2) \cdot cos(\phi_R + \theta_1 + \theta_2)\end{aligned} \quad (5)$$

If the next inequality is not satisfied, then the target is outside the manipulator reach and thus the mobile platform must move in order to bring the target into the manipulator's workspace.

$$\begin{aligned}&|cos(\phi_R)| \leqslant 1 \Rightarrow \\ &\Rightarrow (x_E - x_M)^2 + (y_E - y_M)^2 \leqslant (L_1 + L_2)^2\end{aligned} \quad (6)$$

The first constraint accounts for the nonholonomic behavior of the wheels. It constrains the velocity of the WMR to be along the rolling direction of the wheels only. Velocity perpendicular to the rolling direction must be zero as follows :

$$\dot{x}_R \cdot sin(\phi_R) - \dot{y}_R \cdot cos(\phi_R) = 0 \quad (7)$$

This constraint, written for the manipulator attachment point M, becomes:

$$\dot{x}_R \cdot sin(\phi_R) - \dot{y}_R \cdot cos(\phi_R) + \dot{\phi_R} \cdot D = 0 \quad (8)$$

3 SLIDING-MODE CONTROLLER DESIGN

A WMM system is especially useful when the manipulator task is outside the manipulator reach. Therefore, in this section we assume that this is always the case, in other words that inequality (6) is not satisfied for a given target.

In this chapter is developed a control routine for the mobile robot that allows for independent control of both the task-space (end-effector) and the configuration-space (mobile base). As mentioned before the primary task is controlling the position of the end-effector and attached payload. The trajectory of the mobile base consists of a time varying function of the position of the end-effector. Once the end-effector final position is known, there exists extra degrees-of-freedom that need to be controlled. These consist of the posture of the mobile robot base and arms. This is depicted in Figure 3, where a mobile robot is shown moving from initial position to the final position.

Assumption: The prescribed final posture (position, $[x_E, y_E]$ and orientation $[\phi_R, \theta_1, \theta_2]$) is required.

Although the final position is reachable, it is virtually impossible to harvest exact orientations via continuous feedback controllers at the equilibrium point

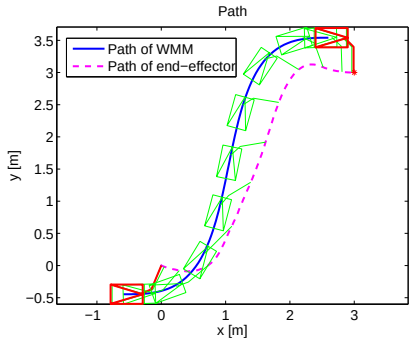

Figure 3: Maneuver example using WMM.

of nonholonomic systems, a direct result of Brockets Theorem (Brockett, 1983). Notwithstanding the limitation, we adopt the sliding-mode technique from (Solea and Cernega, 2009) to maneuver the WMM into a final position such that the prescribed final orientation could also be accomplished.

A trajectory planner for wheeled mobile manipulators must generate smooth velocity profiles (linear and angular) with low associated accelerations. The trajectory planning process can be divided into two separate parts. First, a continuous collision-free path is generated. In a second step, called trajectory generation, a velocity profile along the path is determined. A method to generate a velocity profile, respecting human body comfort, for any two-dimensional path in static environments was proposed in (Solea and Nunes, 2007).

Uncertainties which exist in real mobile robot applications degrade the control performance significantly, and accordingly, need to be compensated. In this section, is proposed a sliding-mode trajectory-tracking controller, in Cartesian space, where trajectory-tracking is achieved even in the presence of large initial pose errors and disturbances. The application of SMC strategies in nonlinear systems has received considerable attention in recent years. A well-studied example of a non-holonomic system is a WMM that is subject to the rolling without slipping constraint. In trajectory tracking is an objective to control the nonholonomic WMM to follow a desired trajectory, with a given orientation relatively to the path tangent, even when disturbances exist.

Let us define the sliding surface $S = [s_1, s_2, s_3, s_4]^T$ as:

$$\begin{aligned}s_1 &= \dot{x}_e + \gamma_x \cdot x_e \\ s_2 &= \dot{y}_e + \gamma_y \cdot y_e + \gamma_0 \cdot sgn(y_e) \cdot \phi_e \\ s_3 &= \dot{\theta}_{e1} + \gamma_{\theta_1} \cdot \theta_{e1} \\ s_4 &= \dot{\theta}_{e2} + \gamma_{\theta_2} \cdot \theta_{e2}\end{aligned} \quad (9)$$

where γ_0, γ_x, γ_y, γ_{θ_1} and γ_{θ_2} are positive constant parameters, x_e, y_e ϕ_e, θ_{e1} and θ_{e2} are the trajectory-tracking errors defined in Fig. 4:

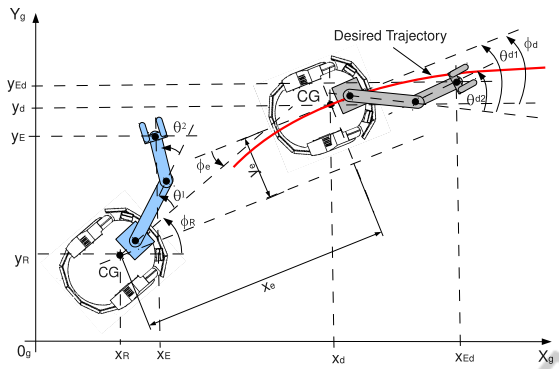

Figure 4: Lateral, longitudinal and orientation errors for WMM.

$$
\begin{aligned}
x_e &= (x_R - x_d)\cdot cos(\phi_d) + (y_R - y_d)\cdot sin(\phi_d)\\
y_e &= -(x_R - x_d)\cdot sin(\phi_d) + (y_R - y_d)\cdot cos(\phi_d)\\
\phi_e &= \phi_R - \phi_d\\
\theta_{e1} &= \theta_1 - \theta_{d1}\\
\theta_{e2} &= \theta_2 - \theta_{d2}
\end{aligned}
\tag{10}
$$

If s_1 converges to zero, trivially x_e converges to zero. If s_2 converges to zero, in steady-state it becomes $y_e = \gamma_y \cdot y_e \gamma_0 \cdot sgn(y_e)\cdot\phi_e$. For $y_e < 0 \Rightarrow \dot{y}_e > 0$ if only if $\gamma_0 < \gamma_y \cdot |y_e|/|\phi_e|$. For $y_e > 0 \Rightarrow \dot{y}_e < 0$ if only if $\gamma_0 < \gamma_y \cdot |y_e|/|\phi_e|$. Finally, it can be known from s_2 that convergence of y_e and $\dot{y}_e$ leads to convergence of ϕ_e to zero. If s_3, s_4 converges to zero, trivially $\theta_e 1$, $\theta_e 2$ converges to zero.

The reaching law is a differential equation which specifies the dynamics of a switching function S. Gao and Hung (Gao and J., 1993) proposed a reaching law which directly specifies the dynamics of the switching surface by the differential equation

$$\dot{s}_i = -p_i \cdot s_i - q_i \cdot sgn(s_i) \tag{11}$$

where $p_i > 0$, $q_i > 0$, $i = 1,2,3,4$.

By adding the proportional rate term $p_1 \cdot s_i$, the state is forced to approach the switching manifolds faster when s is large. It can be shown that the reaching time is finite, and is given by:

$$T_i = \frac{1}{p_i} \cdot ln \frac{p_i \cdot |s_i| + q_i}{q_i} \tag{12}$$

From the time derivative of (9) and using the reaching laws defined in (11) yields:

$$
\begin{aligned}
\ddot{x}_e + \gamma_x \cdot \dot{x}_e &= -p_1 \cdot s_1 - q_1 \cdot sgn(s_1)\\
\ddot{y}_e + \gamma_y \cdot \dot{y}_e + \gamma_0 \cdot sgn(y_e)\cdot\dot{\phi}_e &= -p_2 \cdot s_2 - q_2 \cdot sgn(s_2)\\
\ddot{\theta}_{e1} + \gamma_{\theta_1} \cdot \dot{\theta}_{e1} &= -p_3 \cdot s_3 - q_3 \cdot sgn(s_3)\\
\ddot{\theta}_{e2} + \gamma_{\theta_2} \cdot \dot{\theta}_{e2} &= -p_4 \cdot s_4 - q_4 \cdot sgn(s_4)
\end{aligned}
\tag{13}
$$

From (2), (5) (10) and (13), and after some mathematical manipulation, we get the output commands

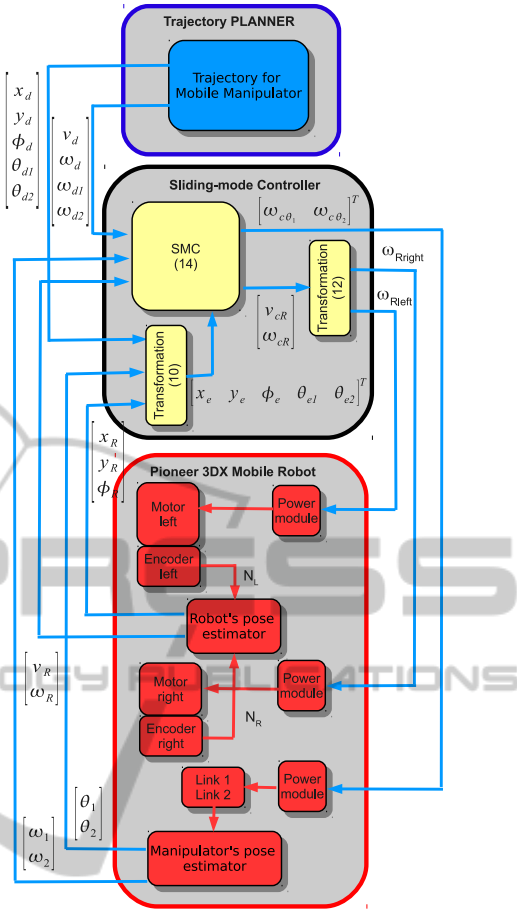

Figure 5: Sliding-mode trajectory tracking control architecture for WMM.

of the sliding-mode trajectory-tracking controller:

$$
\begin{aligned}
\dot{v}_{cR} &= \tfrac{1}{cos(\phi_e)} \cdot (-p_1 \cdot s_1 - q_1 \cdot sgn(s_1) - \gamma_x \cdot \dot{x}_e -\\
&-y_e \cdot \dot{\omega}_d - \dot{y}_e \cdot \omega_d + v_R \cdot \dot{\phi}_e \cdot sin(\phi_e) + \dot{v}_d)\\
\omega_{cR} &= \tfrac{1}{v_R \cdot cos(\phi_e) + \gamma_0 \cdot sgn(y_e)} \cdot (-p_2 \cdot s_2 - q_2 \cdot sgn(s_2) -\\
&-\gamma_y \cdot \dot{y}_e - \dot{v}_r \cdot sin(\phi_e) + x_e \cdot \dot{\omega}_d + \dot{x}_e \cdot \omega_d) + \omega_d\\
\dot{\omega}_{c\theta_1} &= -p_3 \cdot s_3 - q_3 \cdot sgn(s_3) - \gamma_{\theta_1} \cdot \dot{\theta}_{e1}\\
\dot{\omega}_{c\theta_2} &= -p_4 \cdot s_4 - q_4 \cdot sgn(s_4) - \gamma_{\theta_2} \cdot \dot{\theta}_{e2}
\end{aligned}
\tag{14}
$$

The signum functions in the control laws were replaced by saturation functions, to reduce the chattering phenomenon (Slotine and Li, 1991).

4 SIMULATIONS AND RESULTS

In this section, simulation results for the proposed sliding-mode controllers are presented. The simulation are performed in Matlab/Simulink environment to verify behavior of the controlled system. The parameters of the WMM model were chosen to corre-

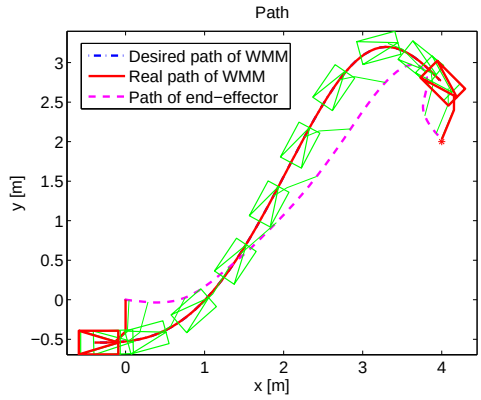

Figure 6: Scenario 1 - Path of mobile manipulator.

spond as closely as possible to the real experimental robot presented in Fig. 1 in the following manner: D = 0.25 [m], L_1 = 0.20 [m], L_2 = 0.40 [m], b = 0.04 [m], r = 0.04 [m]. Wheel velocity commands, are sent to the power modules of the follower mobile robot, and encoder measures N_R and N_L are received in the robots pose estimator for odometric computations.

$$\omega R_{right} = \frac{v_{cR} + b \cdot \omega_{cR}}{r};\ \omega R_{left} = \frac{v_{cR} - b \cdot \omega_{cR}}{r} \quad (15)$$

Figure 5 shows a block diagram of the proposed sliding-mode controller.

4.1 Scenario 1

The first scenario captures a situation where have to maneuver the WMM from an initial to a final state without pose error. The corresponding states and workspace of the simulation are tabulated below (see Table 1).

Table 1: Initial and final pose - Scenario 1.

Name	Value
Initial position of end-effector	$x_E = 0, y_E = 0$
Initial angular position	$\phi_R = 0, \theta_1 = \pi/4, \theta_2 = \pi/4$
Final position of end-effector	$x_E = 4, y_E = 2$
Final angular position	$\phi_R = -\pi/4, \theta_1 = -\pi/4, \theta_2 = -\pi/8$

4.2 Scenario 2

The second scenario captures a situation where have to maneuver the WMM from an initial to a final state with initial pose error. The corresponding states and workspace of the simulation are tabulated below (see Table 2).

The results of the Scenario 2 are given in Figures 9 - 11. Figure 9 shows the desired and real trajectory of the mobile platform and the real trajectory of the end-effector. In figures 10 presents the desired and real

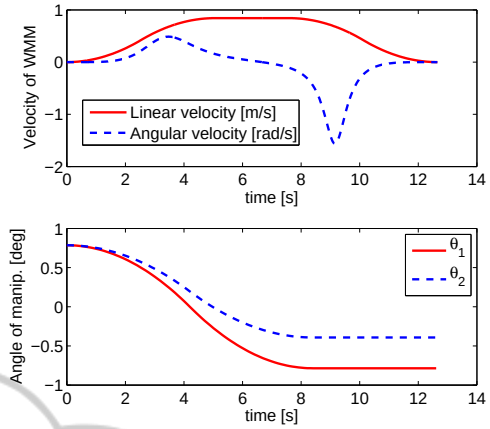

Figure 7: Scenario 1 - Desired velocities for WMM and the relative angles for first and second link of the manipulator.

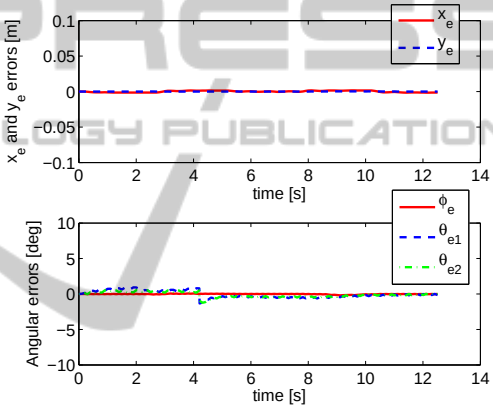

Figure 8: Scenario 1 - Evolution of the errors.

Table 2: Initial and final pose - Scenario 2.

Name	Value
Initial pos. of end-effector	$x_E = 0, y_E = 0$
Initial angular position	$\phi_R = 0, \theta_1 = \pi/8, \theta_2 = -\pi/4$
Final pos. of end-effector	$x_E = 3, y_E = 3$
Final angular position	$\phi_R = 0, \theta_1 = \pi/4, \theta_2 = -\pi/8$
Initial pose errors of WMM	$x_e = -0.20, y_e = -0.6$

velocities (linear and angular) of mobile platform. In Fig. 11 one can observe the performances of sliding-mode controllers. All the initial errors asymptotically converge to zero, as shown in Fig. 11.

5 CONCLUSIONS

In this paper, we will extend the results in [18] to multiple unanchored 2-link ma- nipulators, utilizing again the the sliding-mode control scheme. This control scheme provides a simple but effective means of harnessing control laws of nonlinear systems.

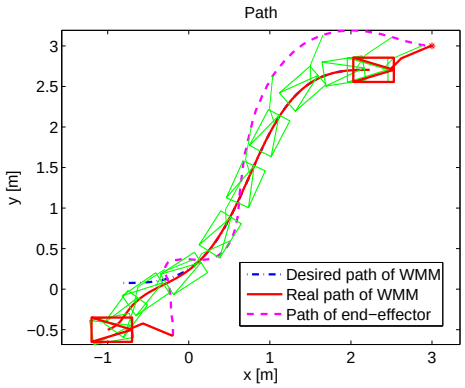

Figure 9: Scenario 2 - Path of mobile manipulator.

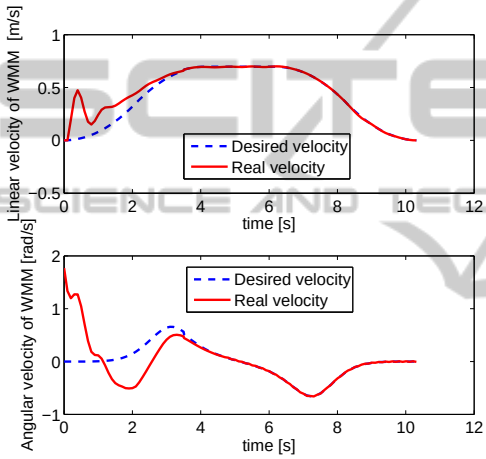

Figure 10: Scenario 2 - Desired and real velocities for WMM.

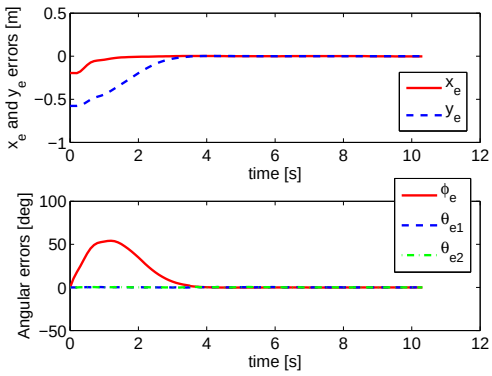

Figure 11: Scenario 2 - Evolution of the errors.

The framework developed here lends itself well to implementations on larger systems with further addition of mobile manipulator modules.

In future work, motivated by this work, we consider the situation when multiple mobile manipulators are grasping an object in a cooperative manner. The purpose of controlling such coordinated system is to control the object in the desired motion.

ACKNOWLEDGEMENTS

This work was supported by CNCSIS-UEFISCSU, project PNII-IDEI 506/2008.

REFERENCES

Bayle, B., Fourquet, J.-Y., Lamiraux, F., and Renaud, M. (2002). Kinematic control of wheeled mobile manipulators. *Proceedings of the 2002 IEEE/RSJ International Conference on Intelligent Robots and Systems*, 1:1572–1577.

Brockett, R. W. (1983). Asymptotic stability and feedback stabilization. In Brockett, R., Millman, R., and Sussmann, H. J., editors, *Differential Geometric Control Theory*, pages 181–191. Birkhauser, Boston.

Fruchard, M., Morin, P., and Samson, C. (2005). A framework for the control of nonholonomic mobile manipulators. *Rapport De Recherche INRIA*, 5556:1–52.

Gao, W. and J., H. (1993). Variable structure control of nonlinear systems: A new approach. *IEEE Transactions on Industrial Electronics*, 40(1):45–55.

Klancar, G., Matko, D., and Blazic, S. (2009). Wheeled mobile robots control in a linear platoon. *Journal of Intelligent and Robotic Systems*, 54(5):709–731.

Kolmanovsky, I. and McClamroch, N. (1995). Developments in nonholonomic control problems. *IEEE Control Systems Magazine*, 15(6):20–36.

Luca, A. D., Oriolo, G., and Giordano, P. R. (2010). Kinematic control of nonholonomic mobile manipulators in the presence of steering wheels. *IEEE International Conference on Robotics and Automation*, pages 1792–1798.

Mazo, M., Speranzon, A., Johansson, K., and Hu, X. (2004). Multi-robot tracking of a moving object using directional sensors. *IEEE International Conference on Robotics and Automation - ICRA 2004*, 2:1103–1108.

Murray, R. M. (2007). Recent research in cooperative control of multi-vehicle systems. *Journal of Dynamic Systems, Measurement and Control*, 129(5):571–583.

Seraji, H. (1993). An on-line approach to coordinated mobility and manipulation. *Proceedings of the 1993 IEEE International Conference on Robotics and Automation*, 1:28–35.

Sharma1, B. N., Vanualailai, J., and Prasad, A. (2010). Trajectory planning and posture control of multiple mobile manipulators. *International Journal of Applied Mathematics and Computation*, 2(1):11–31.

Slotine, J. and Li, W. (1991). *Applied Nonliner Control*. Prentice Hall, New Jersey.

Solea, R. and Cernega, D. (2009). Sliding mode control for trajectory tracking problem - performance evaluation. In *ICANN (2)*, volume 5769 of *Lecture Notes in Computer Science*, pages 865–874. Springer.

Solea, R. and Nunes, U. (2007). Trajectory planning and sliding-mode control based trajectory-tracking for cybercars. *Integrated Computer-Aided Engineering*, 14(1):33–47.

Tang, C. P., Miller, P. T., Krov, V. N., Ryu, J.-C., and Agrawal, S. K. (2008). Kinematic control of a nonholonomic wheeled mobile manipulator - a differential flatness aproach. *Proceedings of ASME Dynamic Systems and Control Conference*, pages 1–8.

Tanner, H. G., Loizou, S., and Kyriakopoulos, K. J. (2003). Nonholonomic navigation and control of cooperating mobile manipulators. *IEEE Transactions on Robotics and Automation*, 19(1):53–64.

Zavlanos, M. and Pappas, G. (2008). Dynamic assignment in distributed motion planning with local coordination. *IEEE Transaction on Robotics*, 24(1):232–242.